Title

Amphetamine pretreatment blunts dopamine-induced D2/D3-receptor occupancy by an arrestin-mediated mechanism: A PET study in internalization compromised mice.

Authors

Mandeville, Joseph
Wey, Hsiao-Ying
Chen, Yin-Ching
et al.

Publication Date

2023-12-01

DOI

10.1016/j.neuroimage.2023.120416

Peer reviewed

HHS Public Access

Author manuscript

Neuroimage. Author manuscript; available in PMC 2024 February 05.

Published in final edited form as:

Neuroimage. 2023 December 01; 283: 120416. doi:10.1016/j.neuroimage.2023.120416.

Amphetamine pretreatment blunts dopamine-induced D2/D3-receptor occupancy by an arrestin-mediated mechanism: A PET study in internalization compromised mice

Joseph B. Mandeville[a,b,*], **Jonah Weigand-Whittier**[a,c], **Hsiao-Ying Wey**[a,b], **Yin-Ching I. Chen**[a,b]

[a]Athinoula A. Martinos Center for Biomedical Imaging, Department of Radiology, Massachusetts General Hospital, Boston, MA, USA

[b]Harvard Medical School, Boston, MA, USA

[c]Department of Bioengineering, University of California, Berkeley, CA, USA

Abstract

While all reversible receptor-targeting radioligands for positron emission tomography (PET) can be displaced by competition with an antagonist at the receptor, many radiotracers show limited occupancies using agonists even at high doses. [^{11}C]Raclopride, a D2/D3 receptor radiotracer with rapid kinetics, can identify the direction of changes in the neurotransmitter dopamine, but quantitative interpretation of the relationship between dopamine levels and radiotracer binding has proven elusive. Agonist-induced receptor desensitization and internalization, a homeostatic mechanism to downregulate neurotransmitter-mediated function, can shift radioligand-receptor binding affinity and confound PET interpretations of receptor occupancy. In this study, we compared occupancies induced by amphetamine (AMP) in drug-naive wild-type (WT) and internalization-compromised β-arrestin-2 knockout (KO) mice using a within-scan drug infusion to modulate the kinetics of [^{11}C]raclopride. We additionally performed studies at 3 h following AMP pretreatment, with the hypothesis that receptor internalization should markedly attenuate occupancy on the second challenge, because dopamine cannot access internalized receptors. Without prior AMP treatment, WT mice exhibited somewhat larger binding potential than KO mice but similar AMP-induced occupancy. At 3 h after AMP treatment, WT mice exhibited binding potentials that were 15 % lower than KO mice. At this time point, occupancy was preserved in KO mice but suppressed by 60 % in WT animals, consistent with a model in which most receptors contributing to binding potential in WT animals were not functional. These

*Corresponding author. jbm@nmr.mgh.harvard.edu (J.B. Mandeville).

CRediT authorship contribution statement

Joseph B. Mandeville: Conceptualization, Methodology, Investigation, Software, Formal analysis, Writing – original draft, Writing – review & editing. **Jonah Weigand-Whittier:** Investigation, Methodology, Writing – review & editing. **Hsiao-Ying Wey:** Conceptualization, Writing – review & editing. **Yin-Ching I. Chen:** Conceptualization, Methodology, Investigation, Writing – review & editing.

Declaration of Competing Interest

None.

results demonstrate that arrestin-mediated receptor desensitization and internalization produce large effects in PET [^{11}C]raclopride occupancy studies using agonist challenges.

Keywords

PET; Dopamine; Internalization; β-arrestin-2; Knock-out; Mice

1. Introduction

Positron emission tomography (PET) measurements infer receptor occupancies through changes in binding potentials associated with a drug or task, but binding potentials depend upon both available receptor concentrations and ligand-receptor affinities. Agonist-induced receptor desensitization and internalization, well established phenomena in vitro (Kang et al., 2014), can cause shifts in ligand-receptor affinity that cloud the interpretation of PET-based measurements of occupancy by simultaneously changing both the concentration of available receptors and the binding affinity to a subset of the receptors. Although receptor trafficking is a leading hypothesis to explain why many PET radioligands are readily displaced by antagonists but exhibit poor sensitivity or even paradoxical increases in binding under agonist conditions (Bantick et al., 2004; Laruelle, 2000; Quelch et al., 2014a), the quantitative impact of this phenomenon in vivo is controversial.

All neuroreceptors appear to be subject to agonist-induced trafficking, but D2/D3 receptors have been a template for studies of this effect on PET binding due to the success of the radioligand [^{11}C] raclopride and the failure of a first generation spiperone derivative, [^{11}C]NMSP, for detecting dopamine release using PET occupancy; in fact, most reports showed that elevation of dopamine produced paradoxical increases in spiperone binding (Chugani et al., 1988; Laruelle, 2000). An agonist-induced increase in binding potential could result from a shift in ligand-receptor affinity due to internalization, which operates on a time scale of minutes (Guo et al., 2010), and binding contributions from a baseline reservoir of internalized receptors could blunt sensitivity to dopamine release. However, internalization is difficult to investigate in vivo, and mechanistic studies in vitro and *ex vivo* have produced disparate results. One study used subcellular fractionation and reported that intracellular receptors were accessible by spiperone but not raclopride (Sun et al., 2003), another used the same method and found that the spiperone exhibited moderately more intracellular binding than raclopride (Quelch et al., 2014b), and a third report found that these radioligands exhibit similarly reduced affinity for internalized receptors (Guo et al., 2010). Thus, mechanistic studies have not converged an explanation for why raclopride but not spiperone is sensitive to dopamine release, or why many other radioligands are insensitive to neurotransmitter release.

Several phenomena from the [^{11}C]raclopride literature could result from desensitization and internalization. Dopamine-induced binding is depressed somewhat longer than would be expected based upon the conjunction of microdialysis data and a simple occupancy model (Laruelle et al., 1997). Simultaneous PET and fMRI data show a temporal divergence, in which the fMRI signal rapidly attenuates for agonist (Sander et al., 2016) but not

antagonist (Sander et al., 2013) stimuli at D2/D3 receptors; although fMRI is an indirect marker of neural activity, these responses match expectations based upon agonist-induced downregulation of receptor functionality. The largest doses of amphetamine produce occupancies of only about 50 % (Laruelle, 2000), an effect that has commonly been attributed to surface receptors with low-affinity for agonists (Caravaggio et al., 2021; Shotbolt et al., 2012) but that also might result from an internalized basal pool of receptors (Quelch et al., 2014b) or even a dynamic shift in affinities due to trafficking that occurs in response to the drug challenge.

Genetically modified mice provide an avenue to test mechanistic hypotheses that would be otherwise difficult to address using noninvasive neuroimaging. β-arrestins are ubiquitous regulators of agonist-induced internalization of G-protein-coupled receptors in the central nervous system (Shenoy and Lefkowitz, 2011). In particular, β-arrestin-2 has been implicated as a primary mediator of D2 receptor endocytosis (Skinbjerg et al., 2009). Using β-arrestin-2 knock-out (KO) mice, one study (Skinbjerg et al., 2010) showed that the D2 agonist [^{11}C]MNPA and the D2 antagonist [^{18}F]fallypride each exhibited somewhat faster recovery of binding potentials at 4 h in mice lacking β-arrestin-2 relative to wild-type (WT) mice. A second study employed fMRI in this same mouse model and observed a slightly more rapid attenuation of response to the dopamine agonist apomorphine in WT animals, which could result from arrestin-mediated receptor downregulation (Sahlholm et al., 2017).

The persistence of depressed binding observed across numerous studies motivated “late-phase” imaging to test the hypothesis that D2 receptor internalization is impaired in schizophrenic patients (Weinstein et al., 2017), but results did not differentiate the patient group when using [^{11}C]raclopride to measure post-stimulant depression of radioligand binding. One drawback of late-phase imaging is that most radioligands, which are selected for crossing lipophilic membranes, probably can access internalized receptors, albeit with modified affinity relative to receptors on the cell surface; in vitro data have both supported (Guo et al., 2010; Quelch et al., 2014b) and refuted (Sun et al., 2003) this hypothesis. If both internalized and externalized receptors contribute to measurements of binding potential, this will partially conceal effects of receptor trafficking using measurements of binding potential alone. Thus it’s possible that the small effect size reported previously using late-phase imaging to differentiate WT and β-arrestin-2 KO mice, together with the success of radiotracers like [^{11}C]raclopride for detecting neurotransmitter release, have obscured the magnitude of internalization-associated effects on PET measurements of occupancy.

Because occupancy is the metric of interest for assessing dopamine release, we undertook direct measurements of dopamine occupancy using a within-scan AMP challenge to quantify [^{11}C]raclopride kinetics in WT and internalization-deficient mice. We hypothesized that a second injection of AMP would produce a larger response in internalization-deficient mice than in WT mice, because only high-affinity external receptors should contribute to the acute response to elevated dopamine, which cannot access internalized receptors. Moreover, we assessed whether [^{11}C]raclopride would show more rapid recovery of binding potential in KO mice, consistent with the one prior study using different radiotracers (Skinbjerg et al., 2010).

2. Methods

PET/MR scans were performed in 50 male mice (13 ± 3 weeks of age, 27 ± 4 g) using a Bruker 4.7T BioSpec MRI scanner with a PET insert (Bruker Biospin Corp., Billerica MA). Wild-type (WT, $n = 26$) and β–arrestin-2 knockout (KO, $n = 24$) mice, obtained from Jackson Laboratory (Bar Harbour, ME), were compared using simultaneous multi-mouse scanning ($n = 6$ per study) by PET/MRI. Prior to scanning, animals were divided into two groups: group "pre-AMP" ($n = 19$) received AMP (3 mg/kg, i.p.) at 2.5 h prior to scanning, while a "naïve" group received no AMP. Two tail vein catheters were then implanted in most mice and observed to be patent ($n = 33$). When two tail veins were available, we used a within-scan challenge paradigm (Fig. 1b); otherwise, studies only assessed baseline binding potentials. Table 1 shows the number of WT and KO animals in each group which were used for assessing the persistence of binding potential after the initial dose of AMP and the functionality of D2/D3 receptors to a subsequent dose of AMP. In all but one case, WT and KO animals were evenly balanced within scans, and positions within the multi-subject bed were counterbalanced by genotype. All procedures were approved by and complied with the regulations of the Institutional Animal Care and Use Committees (IACUC) at Massachusetts General Hospital and the Association for Assessment and Accreditation of Laboratory Animal Care (accreditation number 000809), and results are reported according to ARRIVE guidelines.

Following placement of tail vein catheters, animals were positioned in a custom multi-mouse cradle, and anesthesia was maintained with 1–1.5 % isoflurane in oxygen-enriched air through a multiplexed delivery system. Heating was maintained by warm air blown into the scanner bore, and temperature and respiration were monitored from one mouse per study (Small Animal Instruments Inc., Stony Brook NY). Anesthesia was adjusted to maintain about 60 breaths per minute.

To measured D2/D3 binding potentials, we injected [^{11}C]raclopride (11 ± 3 MBq) at the beginning of each scan using sequential boluses (150 uL) followed by saline flushes of the same amount. At 35–37 min into the scan for all mice with double tail vein catheters, a challenge dose of 1 mg/kg AMP was injected. During the 90-minute PET scan, T2-weighted anatomical MRI scans were collected to enable image registration of individual subjects.

PET data were corrected for scatter and decay but not attenuation and reconstructed by an iterative vendor-supplied algorithm, the maximum-likelihood expectation-maximization (MLEM) method with 12 iterations and a final reconstructed resolution of 0.5 mm in each dimension. Brain volumes were registered to an MRI template volume (Ma et al., 2014) using an affine transformation based upon mutual information with the session-specific MR data, and alignment matrices were applied to create subject-specific four-dimensional PET time-activity profiles within the standardized space. Finally, PET data were analyzed by a pseudo-linear variant of the simplified reference tissue model (Alpert et al., 2003; Ichise et al., 2003) including a constant challenge term, as shown in Fig. 1b. This method derives a measurement of the baseline potential, BP_{ND}, relative to nondisplaceable activity in the reference region (cerebellum) and also enables determination of the change ΔBP_{ND} due to injection of amphetamine.

High uptake of radioligand was observed in the Harderian Glands (HG), consistent with prior reports (Thanos et al., 2002), and injection of amphetamine caused an increase in apparent binding potential in HG, opposite in direction to that seen in caudate putamen (CPu) due to dopamine release. Partial volume contamination from HG was most apparent in animals pretreated with AMP, because prior administration of AMP suppressed binding of radioligand in CPu but not HG. To address this issue, we employed two methods for partial volume correction (PVC) based upon the nominal point-spread-function of 1 mm for this system (Gsell et al., 2020). The first method, which is employed for Figs. 3-5 and all statistical calculations, takes advantage of prior information by anatomically segmenting data to create a region-based correction (Fig. 2c) following the standard geometric transfer matrix (GTM) formalism (Erlandsson et al., 2012). This approach reduces voxel-wise data to one region-of-interest measurement per subject for bilateral CPu. The second method, which is used only for the descriptive Fig. 2, combines the GTM method with three-dimensional uniform cubic b-spline functions to produce anatomically unbiased voxel-based images. Both methods operate on each PET frame to produce a corrected four-dimensional time-activity dataset for each subject.

Group data were analyzed separately for BP_{ND} (n = 50 subjects) and the change in BP_{ND} induced by AMP (n = 35 subjects). We employed a multi-linear analysis including effects for genotype, AMP injection, and the interaction of genotype and AMP injection. Additionally, we computed receptor occupancy for each animal with two tail catheters as the percentage change in binding potential, and the compared occupancies versus genotype using a T test.

To interpret results, we assumed that the primary difference between KO and WT animals was due to post-synaptic receptor desensitization and internalization. Accordingly, we applied a classical occupancy model to interpret data in KO animals, and we allowed for internalization in WT animals. Each cohort provides three independent binding ratios (i.e., four binding potentials). Each ratio can be described in terms of the fraction of bound receptors (b), the fraction of unbound internalized receptors (i), and the affinity shift for internalized relative to surface receptors (a) as

$$\frac{BP_{ND}^{(1)}}{BP_{ND}^{(0)}} = \frac{(1 - b_1 - i_1) + ai_1}{(1 - b_0 - i_0) + ai_0} \quad (1)$$

For KO animals, we assumed $i_0 = i_1 = 0$, and we described the three binding ratios in terms of external bound receptors (occupancies). For WT animals, we constrained external occupancies to match values obtained in KO animals, under the assumption of similar dopamine release in the two cohorts, and we computed the three internalization fractions needed to describe the three binding ratios. For unmeasured values, we assumed a basal D2 receptor occupancy of 20 %, which represents an average of literature values (Mandeville et al., 2013), and an internalization shift of 0.45 (Guo et al., 2010).

3. Results

Fig. 2 provides descriptive results by group in the form of voxel-based maps after PVC. In WT mice, the highest subject-averaged values of BP_{ND} in striatum in WT mice were about 4 without PVC and 6 after voxel-based PVC. KO mice showed lower average values of BP_{ND} than WT mice, whereas AMP-pretreated KO mice showed a larger absolute response of ΔBP_{ND} than AMP-pretreated WT mice.

Fig. 3 shows group averages for BP_{ND} in CPu as a function of genotype and pretreatment. Naïve KO mice exhibited a slightly lower BP_{ND} than naïve WT mice ($p<0.05$). At 3 h after pretreatment by AMP, both WT and KO mice exhibited highly significant suppression of BP_{ND} ($p<0.001$), but BP_{ND} was not differentiated by genotype at this time point. A multi-linear model (Fig. 3b) found significant effects of genotype ($p<0.01$), pretreatment by AMP ($p<0.001$), and the interaction of genotype and AMP pretreatment ($p<0.05$). In the figure, color bars show the range of each effect as one standard error from the mean; a negative value corresponds to a reduction of BP_{ND} by the labeled effect, and a positive value means the effect was associated with higher values of BP_{ND}. This analysis shows that KO animals exhibited more recovery at 3 h after AMP treatment than WT animals, relative to the respective naïve baselines.

Fig. 4 repeats the same analysis on the acute AMP-induced response, ΔBP_{ND}. Consistent with the larger BP_{ND} in WT relative to KO mice, WT mice exhibited higher ΔBP_{ND} than KO mice in the naïve state ($p<0.05$). At 3 h after pretreatment, a second injection of AMP produced a significantly smaller response in WT mice ($p<0.001$) but not in KO mice. A linear model statistical analysis (Fig. 4b) showed significant effects of genotype ($p<0.05$), AMP pretreament ($p<0.001$), and the interaction of genotype and AMP pretreatment ($p<0.01$). At 3 h after AMP pretreatment, KO animals exhibited a much larger ΔBP_{ND} in response to acute AMP relative to the responses in naïve animals.

Fig. 5 normalizes BP_{ND} and AMP-induced ΔBP_{ND} to average values observed in naïve animals. While BP_{ND} showed slightly more recovery in KO than WT mice at 3 h after pretreatment by AMP, the relative difference in acute responses to a second dose (ΔBP_{ND}) was striking. Amphetamine-induced receptor occupancy (ΔBP_{ND}/ BP_{ND}) is compared in Fig. 5c. KO animals showed a conserved occupancy between naïve and AMP-pretreated states, whereas the acute AMP-induced occupancy in WT animals was reduced to about 40 % of the naïve value ($p<0.05$), suggesting that the binding potential at 3 h after pretreatment of AMP in WT animals was dominated by receptors that were not functional.

The lower panels of Fig. 5 present a model-dependent interpretation of data using Eq. (1). For KO animals, amphetamine increased dopamine occupancies from 20 % to 44 % in the naïve state and from 57 % to 69 % in the post-treatment state. Applying these values to the external receptor occupancies in the WT state, measured data suggested internalization fractions for unbound receptors were 21 %, 48 %, and 59 % in conditions of naïve challenge, AMP-pretreated baseline, and AMP-pretreated challenge, respectively. In other words, data can be described by a model in which KO and WT animals respond similarly to AMP, except that pretreatment by 3 mg/kg AMP (i.p.) internalized about half of

the unbound receptors, blunting the subsequent AMP-induced occupancy 2-fold with respect to either AMP challenge in KO animals or the first AMP challenge in WT animals.

4. Discussion

Insensitive responses to receptor agonists (neurotransmitters or exogenous drugs), or even paradoxical increases binding potentials, have confounded PET occupancy studies for many radiotracers and receptor systems. A leading hypothesis for this effect is receptor desensitization and internalization, a homeostatic mechanism for response downregulation and intracellular signaling. Desensitization and internalization are serial processes in a cascade of downregulation events following prolonged agonist stimulation, with internalization ultimately leading to recycling or degradation of the receptors (Tian et al., 2014). By comparing WT mice to β–arrestin-2 KO mice with compromised D2-receptor internalization, this study showed that KO mice maintain a consistent dopamine occupancy after pretreatement with AMP relative to the naive condition, whereas occupancy is severely reduced in WT mice on a repeated AMP challenge. Moreover, [^{11}C]raclopride binding potentials recover more slowly in the natural state following infusion of AMP, as previously reported for different radiotracers. Both observations are consistent with a differential effect of receptor desensitization and internalization in these two cohorts.

4.1. AMP-induced occupancy in WT and β-arrestin-2 KO mice

Using a within-scan challenge design, our study showed a highly blunted acute response to dopamine on a second challenge several hours of the first administration of a dopamine-elevating stimulant. Because desensitization and internalization are arrestin-mediated processes, the simplest interpretation of the highly attenuated occupancy to a second AMP injection in WT but KO animals is that most receptors that contributed to BP_{ND} at the later time point in WT mice were not functional. Reduced competitive binding after pretreatment with AMP could result either from desensitization, in which a subset of surface receptors converts to lower affinity for binding to agonist (dopamine) but not antagonist (raclopride), or internalization, in which receptors are accessible to radioligand but not dopamine. In either case, a portion of the receptors available to raclopride are inaccessible to dopamine or bind with lower affinity than in the naïve state.

Although our occupancy results did not differ significantly by genotype during the first exposure to AMP, internalization of unbound receptors would be expected to increase the apparent occupancy, as shown by the model fit to data. We assumed no basal pool of internalized receptors; any such pool would require higher internalization fractions than reported here for all states. (Quelch et al., 2014b) estimated the internal pool of D2/D3 receptors at baseline to contribute about 15 % to measurements of binding potential, which would imply an internalized basal pool of about 30 % of the total receptor population if the affinity shift described by (Guo et al., 2010) is correct.

4.2. Persistence of depressed BP_{ND} following AMP treatment

A prior study using [^{11}C]MNPA and [^{11}C]fallypride demonstrated that β–arrestin-2 KO mice exhibited more rapid recovery of binding potential relative to WT mice. Our study

reproduced this result for the commonly used radiotracer [^{11}C]raclopride. Although the use of different radiotracers and time points limits comparisons, in both studies the relative magnitude of the differential effect was small: at the late time point, KO animals exhibited a 15 % greater recovery of binding potentials than WT mice in our study (Fig. 5b) and about a 20 % greater recovery in the earlier study. The late time point selected for our study (3 h between AMP pretreatment and the second challenge dose) was 1.5 h shorter than the earlier study, which presumably explains why we observed less overall recovery in binding potentials relative to the naïve state than the earlier study.

Interpretation of the persistence of BP_{ND} as an index of agonist-induced receptor downregulation is complicated by in vitro data that internalized D2 receptors can be accessed by raclopride, although the binding affinity to these receptors is reduced relative to surface receptors (Guo et al., 2010; Quelch et al., 2014b). If internalized receptors still contribute to measurements of BP_{ND}, this will mask some of the effect of receptor trafficking from the cell membrane surface to endosomes. Presumably, this can explain why BP_{ND} exhibited a much smaller relative effect of genotype in these studies than the occupancy to a repeated challenge.

4.3. Agonist-associated affinity shifts: implications

Our data suggest that contributions from a baseline pool of internalized D2/D3 receptors probably have a larger effect on occupancy than agonist-induced trafficking, which can dynamically modify ligand-receptor affinity. Raclopride, the radioligand employed in this study, has been reported to exhibit a 2-fold reduction in affinity to internalized receptors (Guo et al., 2010), but internalization in principle can also increase affinity through a “trapping” mechanism that prolongs the dissociation time (Chugani et al., 1988). Ligands that exhibit an increase in target affinity following agonist stimulation present an unfortunate paradox for measurement methods, because the two components of binding potential, affinity and receptor availability, change in opposite directions. This mechanism was posited for the spiperone radioligands and analogs, based upon measurements showing agonist-associated increases in the dissociation time constant (Chugani et al., 1988).

Unfortunately, many current PET radioligands that are easily displaced by antagonists, including those targeting D1 receptors or mu opioids (Hume et al., 2007; Laruelle, 2000; Quelch et al., 2014a), show little sensitivity to displacement by endogenous neurotransmitter or even exogenous agonists. If dynamic shifts in affinity underlie this problem, then one would expect insensitive radiotracers to exhibit increased affinity upon internalization, as suggested by the trapping mechanism proposed by (Chugani et al., 1988) for spiperone. However, (Guo et al., 2010) reported similar affinity shifts for three radiotracers (raclopride, spiperone, PHNO) with very different sensitivities to dopamine. The lack of differentiation in affinity shifts between antagonist (e.g., raclopride) and agonist (e.g., PHNO) is perplexing, because receptor are expected to internalize in a low-affinity state (Ko et al., 2002), which would produce an affinity reduction in addition to ligand-dependent environment-specific binding. Thus, the role that affinity shifts play in reducing the sensitivity of many radioligands for neurotransmitter, or in elevating the responsiveness to dopamine for agonist radiotracers like PHNO, remains unsettled.

4.4. Limitations

Although mechanistic inferences from this study presumably pertain to human studies, is likely that internalization-related confounds are smaller in humans due to smaller agonists doses, which are limited for safety reasons. In principle, this paradigm could be employed to reevaluate D2 receptor internalization in schizophrenic versus control subjects (Weinstein et al., 2017) with the hope that a smaller effect size in humans might be partially compensated by a reduction of experimental variance, which is relatively high in mouse models due factors that are difficult to control (e.g., radioactive spillover from Harderian glands, radiotracer mass effects, small injection volumes).

Like most non-invasive imaging studies, this study is limited due to missing information that could only be obtained using invasive methods in additional cohorts. An autoradiographic study reported no significant differences between WT and β–arrestin-2 KO mice in densities of D1 or D2 receptors, dopamine transporters, or vesicular monoamine transporter-2 (Sahlholm et al., 2017). We found that KO mice had a somewhat lower D2/D3 BP_{ND}, and the Sahlholm report found trends for lower levels of both D1 and D2 receptors; these subtle differences could be an adaptation to lower dopaminergic stimulation in the absence of arrestin-mediated downregulation of function.

We did not have a direct measurement of dopamine levels, so it is possible that some differences between WT and KO animals could be explained by different levels of dopamine release. Measured AMP-induced occupancies between cohorts were not different in the naïve state, but internalization associated with β-arrestin-2 could make occupancy an unreliable relative index of dopamine release in the two groups. A possible mechanism for this difference could be agonist-induced desensitization of D2 autoreceptors, which contribute to dopamine regulation. Agonist stimulation desensitizes but does not internalize autoreceptors (Robinson et al., 2017), and desensitized autoreceptors in WT animals could prolong dopamine release relative to KO animals. In principle, this potential difference between cohorts could explain studies that only measure the persistence of binding potentials (Skinbjerg et al., 2010), but downregulation of autoreceptor function would be expected to potentiate WT dopamine release on a repeated challenge and thereby potentiate occupancy, which is opposite the effect seen in this study.

Arrestins mediate D2-receptor internalization (Ito et al., 1999), and β-arrestin-2 KO mice are known to be deficient in D2 receptor internalization (Skinbjerg et al., 2009). However, functional differences between β-arrestins are not well understood, and one study implicated β-arrestin-1 rather than β-arrestin-2 in agonist-induced D2 receptor trafficking (Macey et al., 2004). In other G-protein coupled receptor systems, non-arrestin internalization mechanisms have been reported to contribute to the internalization (Moo et al., 2021). Thus, it is possible that these β-arrestin-2 KO mice maintain some ability to desensitize and internalize D2 receptors.

There are methodological limitations associated with small-animal imaging. The small brains of mice and the limited (1 mm) resolution of PET created regional partial volume contamination; in particular, activity from HG spreading into striatum presented an experimental error that we addressed by a standard correction technique. Prior studies had

worse spatial resolution and did not correct for this source of error (Skinbjerg et al., 2010; Thanos et al., 2002), but errors in the AMP-pretreated portion of our study were relatively larger than in the naïve state due to depression of binding in striatum but not HG. There was no indication, however, that this error differed by genotype. Lacking a suitable system for computed tomography (CT), we did not apply attenuation correction like many other small animals studies, but rather we counterbalanced animal positions in the multisubject cradle. While attenuation should have small effects on occupancy derived from within-subject measurements, absolute errors in multisubject mouse data without attenuation correction have been reported to be about 15 % [ref Habte 2013]. Finally, resolution limitations and limited extra-striatal binding of [^{11}C]raclopride made it not possible to investigate dopamine release outside of striatum.

5. Conclusions

We employed a commonly used D2/D3-receptor radiotracer, [^{11}C] raclopride, to show two phenomena consistent with dopamine-induced receptor trafficking in wild-type animals relative to β-arrestin-2 knockout animals: a prolonged reduction in binding potential and a decreased occupancy to a second dopamine challenge. These results implicate receptor desensitization and internalization as mechanisms that must be considered in the interpretation of PET measurements of occupancy when using direct or indirect agonists. Importantly, this is the first in vivo PET study to show arrestin-mediated effects on receptor occupancy to a second dopamine challenge, which provides further evidence for the influence of internalization on dopamine D2 receptor binding potentials. Moreover, results suggest that radioligand displacement by agonist is highly dependent on the proportion of internalized receptors, a result that has implications for the interpretation of radioligand sensitivity to agonists and the development of next-generation radiotracers.

Acknowledgements

This work was supported by the National Institutes Health (grant numbers R01NS112295, S10RR026666, S10OD023503).

Data availability

Data will be made available on request.

References

Alpert NM, Badgaiyan RD, Livni E, Fischman AJ, 2003. A novel method for noninvasive detection of neuromodulatory changes in specific neurotransmitter systems. Neuroimage 19, 1049–1060. [PubMed: 12880831]

Bantick RA, Rabiner EA, Hirani E, de Vries MH, Hume SP, Grasby PM, 2004. Occupancy of agonist drugs at the 5-HT1A receptor. Neuropsychopharmacology 29, 847–859. [PubMed: 14985704]

Caravaggio F, Porco N, Kim J, Torres-Carmona E, Brown E, Iwata Y, Nakajima S, Gerretsen P, Remington G, Graff-Guerrero A, 2021. Measuring amphetamine-induced dopamine release in humans: a comparative meta-analysis of [(11) C]raclopride and [(11) C]-(+)-PHNO studies. Synapse 75, e22195. [PubMed: 33471400]

Chugani DC, Ackermann RF, Phelps ME, 1988. In vivo [3H]spiperone binding: evidence for accumulation in corpus striatum by agonist-mediated receptor internalization. J. Cereb. Blood Flow Metab 8, 291–303. [PubMed: 2966803]

Erlandsson K, Buvat I, Pretorius PH, Thomas BA, Hutton BF, 2012. A review of partial volume correction techniques for emission tomography and their applications in neurology, cardiology and oncology. Phys. Med. Biol 57, R119–R159. [PubMed: 23073343]

Gsell W, Molinos C, Correcher C, Belderbos S, Wouters J, Junge S, Heidenreich M, Velde GV, Rezaei A, Nuyts J, Cawthorne C, Cleeren F, Nannan L, Deroose CM, Himmelreich U, Gonzalez AJ, 2020. Characterization of a preclinical PET insert in a 7 tesla MRI scanner: beyond NEMA testing. Phys. Med. Biol 65, 245016. [PubMed: 32590380]

Guo N, Guo W, Kralikova M, Jiang M, Schieren I, Narendran R, Slifstein M, Abi-Dargham A, Laruelle M, Javitch JA, Rayport S, 2010. Impact of D2 receptor internalization on binding affinity of neuroimaging radiotracers. Neuropsychopharmacology 35, 806–817. [PubMed: 19956086]

Hume SP, Lingford-Hughes AR, Nataf V, Hirani E, Ahmad R, Davies AN, Nutt DJ, 2007. Low sensitivity of the positron emission tomography ligand [11C] diprenorphine to agonist opiates. J. Pharmacol. Exp. Ther 322, 661–667. [PubMed: 17488881]

Ichise M, Liow JS, Lu JQ, Takano A, Model K, Toyama H, Suhara T, Suzuki K, Innis RB, Carson RE, 2003. Linearized reference tissue parametric imaging methods: application to [11C]DASB positron emission tomography studies of the serotonin transporter in human brain. J. Cereb. Blood Flow Metab 23, 1096–1112. [PubMed: 12973026]

Ito K, Haga T, Lameh J, Sadee W, 1999. Sequestration of dopamine D2 receptors depends on coexpression of G-protein-coupled receptor kinases 2 or 5. Eur. J. Biochem 260, 112–119. [PubMed: 10091590]

Kang DS, Tian X, Benovic JL, 2014. Role of beta-arrestins and arrestin domain-containing proteins in G protein-coupled receptor trafficking. Curr. Opin. Cell Biol 27, 63–71. [PubMed: 24680432]

Ko F, Seeman P, Sun WS, Kapur S, 2002. Dopamine D2 receptors internalize in their low-affinity state. Neuroreport 13, 1017–1020. [PubMed: 12060799]

Laruelle M, 2000. Imaging synaptic neurotransmission with in vivo binding competition techniques: a critical review. J. Cereb. Blood Flow Metab 20, 423–451. [PubMed: 10724107]

Laruelle M, Iyer RN, Tikriti MS, Zea-Ponce Y, Malison R, Zoghbi SS, Baldwin RM, Kung HF, Charney DS, Hoffer PB, Innis RB, Bradberry CW, 1997. Microdialysis and SPECT measurements of amphetamine-induced dopamine release in nonhuman primates. Synapse 25, 1–14. [PubMed: 8987142]

Ma D, Cardoso MJ, Modat M, Powell N, Wells J, Holmes H, Wiseman F, Tybulewicz V, Fisher E, Lythgoe MF, Ourselin S, 2014. Automatic structural parcellation of mouse brain MRI using multi-atlas label fusion. PLoS One 9, e86576. [PubMed: 24475148]

Macey TA, Gurevich VV, Neve KA, 2004. Preferential Interaction between the dopamine D2 receptor and Arrestin2 in neostriatal neurons. Mol. Pharmacol 66, 1635–1642. [PubMed: 15361545]

Mandeville JB, Sander CY, Jenkins BG, Hooker JM, Catana C, Vanduffel W, Alpert NM, Rosen BR, Normandin MD, 2013. A receptor-based model for dopamine-induced fMRI signal. Neuroimage 75, 46–57. [PubMed: 23466936]

Moo EV, van Senten JR, Brauner-Osborne H, Moller TC, 2021. Arrestin-dependent and -independent internalization of G protein-coupled receptors: methods, mechanisms, and implications on cell signaling. Mol. Pharmacol 99, 242–255. [PubMed: 33472843]

Quelch DR, Katsouri L, Nutt DJ, Parker CA, Tyacke RJ, 2014a. Imaging endogenous opioid peptide release with [11C]carfentanil and [3H]diprenorphine: influence of agonist-induced internalization. J. Cereb. Blood Flow Metab 34, 1604–1612. [PubMed: 25005876]

Quelch DR, Withey SL, Nutt DJ, Tyacke RJ, Parker CA, 2014b. The influence of different cellular environments on PET radioligand binding: an application to D2/3-dopamine receptor imaging. Neuropharmacology 85, 305–313. [PubMed: 24910074]

Robinson BG, Bunzow JR, Grimm JB, Lavis LD, Dudman JT, Brown J, Neve KA, Williams JT, 2017. Desensitized D2 autoreceptors are resistant to trafficking. Sci. Rep 7, 4379. [PubMed: 28663556]

Sahlholm K, Ielacqua GD, Xu J, Jones LA, Schlegel F, Mach RH, Rudin M, Schroeter A, 2017. The role of beta-arrestin2 in shaping fMRI BOLD responses to dopaminergic stimulation. Psychopharmacology (Berl.) 234, 2019–2030. [PubMed: 28382543]

Sander CY, Hooker JM, Catana C, Normandin MD, Alpert NM, Knudsen GM, Vanduffel W, Rosen BR, Mandeville JB, 2013. Neurovascular coupling to D2/D3 dopamine receptor occupancy using simultaneous PET/functional MRI. Proc. Natl. Acad. Sci. USA 110, 11169–11174. [PubMed: 23723346]

Sander CY, Hooker JM, Catana C, Rosen BR, Mandeville JB, 2016. Imaging Agonist-Induced D2/D3 Receptor Desensitization and Internalization In Vivo with PET/fMRI. Neuropsychopharmacology 41, 1427–1436. [PubMed: 26388148]

Shenoy SK, Lefkowitz RJ, 2011. beta-Arrestin-mediated receptor trafficking and signal transduction. Trend. Pharmacol. Sci 32, 521–533.

Shotbolt P, Tziortzi AC, Searle GE, Colasanti A, van der Aart J, Abanades S, Plisson C, Miller SR, Huiban M, Beaver JD, Gunn RN, Laruelle M, Rabiner EA, 2012. Within-subject comparison of [(11)C]-(+)-PHNO and [(11)C] raclopride sensitivity to acute amphetamine challenge in healthy humans. J. Cereb. Blood Flow Metab 32, 127–136. [PubMed: 21878947]

Skinbjerg M, Ariano MA, Thorsell A, Heilig M, Halldin C, Innis RB, Sibley DR, 2009. Arrestin3 mediates D(2) dopamine receptor internalization. Synapse 63, 621–624. [PubMed: 19309759]

Skinbjerg M, Liow JS, Seneca N, Hong J, Lu S, Thorsell A, Heilig M, Pike VW, Halldin C, Sibley DR, Innis RB, 2010. D2 dopamine receptor internalization prolongs the decrease of radioligand binding after amphetamine: a PET study in a receptor internalization-deficient mouse model. Neuroimage 50, 1402–1407. [PubMed: 20097293]

Sun W, Ginovart N, Ko F, Seeman P, Kapur S, 2003. In vivo evidence for dopamine-mediated internalization of D2-receptors after amphetamine: differential findings with [3H]raclopride versus [3H]spiperone. Mol. Pharmacol 63, 456–462. [PubMed: 12527818]

Thanos PK, Taintor NB, Alexoff D, Vaska P, Logan J, Grandy DK, Fang Y, Lee JH, Fowler JS, Volkow ND, Rubinstein M, 2002. In vivo comparative imaging of dopamine D2 knockout and wild-type mice with (11)C-raclopride and microPET. J. Nucl. Med 43, 1570–1577. [PubMed: 12411561]

Tian X, Kang DS, Benovic JL, 2014. beta-arrestins and G protein-coupled receptor trafficking. Handb. Exp. Pharmacol 219, 173–186. [PubMed: 24292830]

Weinstein JJ, van de Giessen E, Rosengard RJ, Xu X, Ojeil N, Brucato G, Gil RB, Kegeles LS, Laruelle M, Slifstein M, Abi-Dargham A, 2017. PET imaging of dopamine-D2 receptor internalization in schizophrenia. Mol. Psychiatry

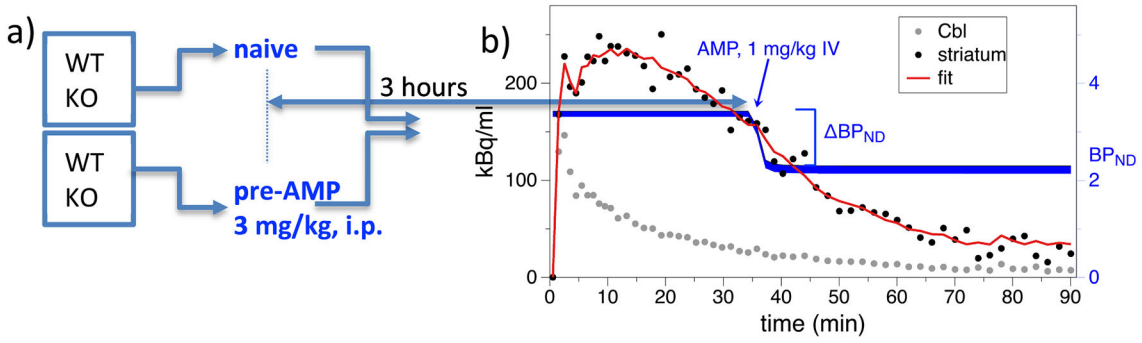

Fig. 1.

Experimental design and analysis. Wild-type (WT) or βarr2-knockout (KO) mice were pretreated with amphetamine (pre-AMP, 3 mg/kg IP) and then scanned by PET following injection of [11C]raclopride. For mice with two implanted tail catheters (n = 33 total), a second injection of AMP (1 mg/kg IV) was delivered at about 35 min into the scan. Data were analyzed using a pseudo-linear model variant of the simplified reference tissue model (SRTM) with inclusion of a single term to enable measurement of non-displaceable binding potential (BP_{ND}) and the AMP-induced shift in this quantity (ΔBP_{ND}, blue error envelope).

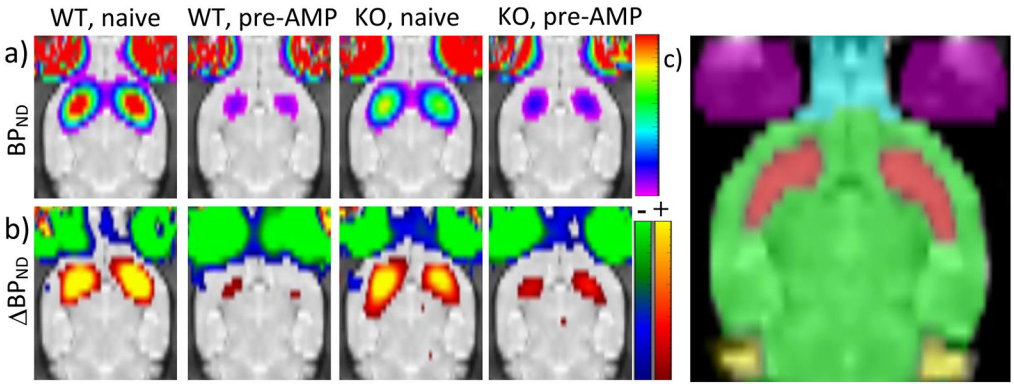

Fig. 2.

Binding potential (a, scale 1.5 to 5) and the AMP-induced changes in binding potential (b, scale 0.2 to 1.2) for wild-type (WT) and βarr2-knockout (KO) mice who were naïve or pretreated with AMP. Voxel-wise partial volume corrections have been applied to all maps. c) To create region-of-interest measurements from bilateral CPu, partial volume corrections were employed using a geometric transfer matrix with MRI-based anatomical segmentation of CPu (red), olfactory bulb (cyan), cerebellum (yellow), and brain remainder (green), plus Harderian glands defined from PET.

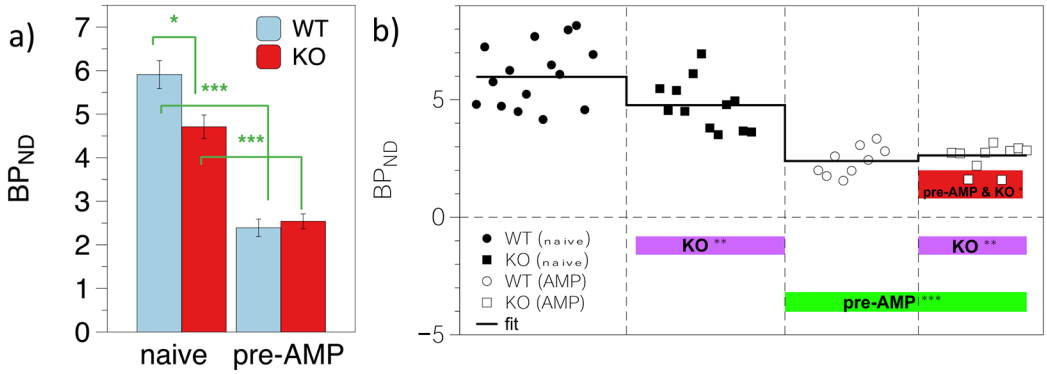

Fig. 3.

Persistence of BP_{ND} following injection of amphetamine (AMP, 3 mg/kg IP) in wild-type (WT) and βarr2 knock-out (KO) mice. a) Group results in drug-naïve and AMP-treated mice at 2.5 h after pretreatment. b) A linear model analysis showing effects of genotype (purple bars, $p<0.01$ **), response to AMP (green bar, $p<<0.001$ ***), and the interaction of genotype and AMP (red bar, $p<0.05$ *). Colored bars span the mean ± standard error of the effect.

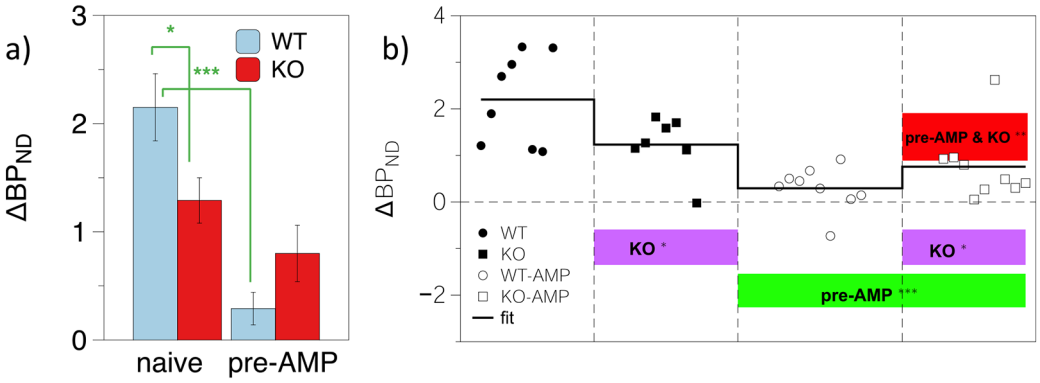

Fig. 4.

Persistence of AMP-induced response (ΔBP_{ND}) following injection of amphetamine (AMP) in wild-type (WT) and βarr2 knock-out (KO) mice. a) Group results in naïve mice and 2.5 h after pretreatment with AMP (3 mg/kg, IP). b) A linear model analysis showing effects of genotype (purple bars, $p<0.05$ *), response to AMP (green bar, $p<0.001$ ***), and the interaction of genotype and AMP (red bar, $p<0.01$ **). Colored bars span the mean ± standard error of the effect.

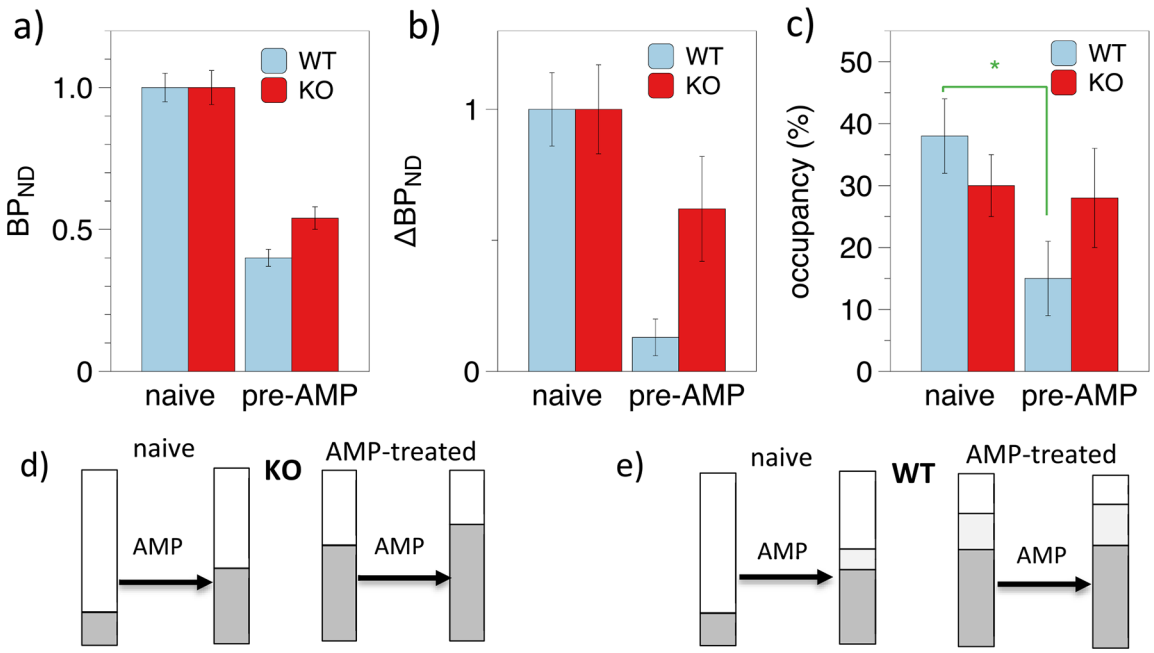

Fig. 5.

Results for BP_{ND} (a) and AMP-induced ΔBP_{ND} (b) normalized to the respective naïve-state value in WT and KO mice. Occupancies (c) showed a significant post-treatment reduction ($p<0.05$) for WT but not KO mice. A model-dependent interpretation is shown in lower panels, using dark gray to indicate bound receptors, light gray to indicate unbound internalized receptors, and white to indicate unbound cell surface receptors. d) A classical occupancy model for KO animals that assumes a 20 % baseline occupancy derives occupancies of 44 %, 57 %, and 69 % in the three other conditions. e) An internalization model for WT animals that is constrained to match dopamine-driven external occupancies in KO mice derives internalization fractions for unbound receptors of 21 %, 48 %, and 59 % in the three non-baseline conditions.

Table 1

Numbers of wild-type (WT) and β-arrestin-2 knock-out (KO) mice used in this study. Animals were either naïve to amphetamine (AMP) or pretreated by AMP (pre-AMP). When two tail catheters were implanted and patent, animals received a dose of AMP as a within-scan challenge to assess ΔBP_{ND}.

Measurement	Pretreatment	WT mice	KO mice
BP_{ND}, ΔBP_{ND}	Naïve	9	8
BP_{ND}, ΔBP_{ND}	Pre-AMP	9	9
BP_{ND} only	Naïve	8	6
BP_{ND} only	Pre-AMP	0	1
Totals		26	24